

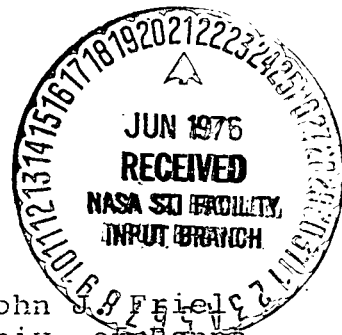
File with  
N76-24684

Imp# 76-42109

FINAL TECHNICAL REPORT

REPRODUCIBLE COPY  
(FACILITY COPY)

Microprobe and Oxygen Fugacity Study of Armalcolite



John J. Friedl  
Univ. of Penna.  
Dept. of Geology  
MSG 7119  
6/14/76

## SUMMARY OF PROJECT

The work performed under NSG 7119 was a continuation of the study of the stability of armalcolite started under NSG 7031. During the period of this grant, the stability of synthetic armalcolite was determined as a function of oxygen fugacity with particular regard to the oxidation state of iron and titanium. The equilibrium pseudobrookite (armalcolite) composition was measured at 1200°C under various conditions of oxidation typical of the lunar environment. These data, when compared with published descriptions of mare basalts, provide information about the conditions of crystallization of armalcolite-bearing lunar rocks.

Some information about the crystal chemistry of armalcolite was obtained from X-ray diffraction and electron microprobe analyses of synthetic armalcolite and Zr-armalcolite. Further data was gathered from a comparison of the Mössbauer spectra of a phase pure stoichiometric armalcolite and one containing appreciable amounts of trivalent titanium.

Both the high pressure work previously discussed<sup>1</sup> and the results of the work performed under this grant are reported in the enclosed manuscript submitted to *Geochimica et Cosmochimica Acta*.

<sup>1</sup>Friel, J. J. (1974) Phase Equilibria Study of Pseudobrookite-Type Minerals. Final Technical Report, NSG 7031.

ARMALCOLITE STABILITY AS A  
FUNCTION OF PRESSURE AND OXYGEN FUGACITY

John J. Friel\*

R. Ian Harker

Department of Geology  
University of Pennsylvania  
Philadelphia, Pennsylvania  
19174

and

Gene C. Ulmer  
Department of Geology  
Temple University  
Philadelphia, Pennsylvania  
19122

\*Present address:  
Department of Metallurgy and  
Materials Science  
Lehigh University  
Bethlehem, Pennsylvania  
18015

## ABSTRACT

The stability of synthetic armalcolite of composition  $(\text{Fe}_{.5}\text{Mg}_{.5})\text{Ti}_2\text{O}_5$  was studied as a function of total pressure up to 15 kb. and  $1200^\circ\text{C}$  and also as a function of oxygen fugacity ( $f\text{O}_2$ ) at  $1200^\circ\text{C}$  and 1 atm. total pressure. The high pressure experiments were done in silver-palladium containers using a piston-cylinder high pressure apparatus. Iron loss to the  $\text{Ag}_{55}\text{Pd}_{45}$  sample containers was shown to be as small as 1.4 wt. % of the total iron content of the charge. Armalcolite broke down to a mixture of rutile plus magnesian ilmenite with  $dP/dT$  positive. A zirconium-armalcolite was synthesized and analyzed, and it was determined that 4% by weight  $\text{ZrO}_2$  appears to saturate armalcolite under these experimental conditions. The similar breakdown of Zr-armalcolite probably occurs at 1 to 2 kb. less pressure than that required for the breakdown of Zr-free armalcolite. The zirconium partitions approximately equally into rutile and ilmenite solid solution. The P-T curves for armalcolite stability show that the maximum depth for the crystallization of lunar armalcolite as a liquidus phase is about 400 km.

The stability of armalcolite as a function of  $f\text{O}_2$  was determined thermogravimetrically at  $1200^\circ\text{C}$  and 1 atm. by weighing sintered pellets of starting material in a controlled atmosphere furnace. Armalcolite,  $(\text{Fe}_{.5}\text{Mg}_{.5})\text{Ti}_2\text{O}_5$ , is stable over a range of  $f\text{O}_2$  from about  $10^{-9.5}$  to  $10^{-10.5}$  atm. Below this range to at least  $10^{-12.8}$  atm. ilmenite plus a reduced armalcolite are formed.

These products were analyzed by Mössbauer spectroscopy and no metallic iron was detected, therefore some of the titanium must have been reduced to  $\text{Ti}^{3+}$ . This reduction may provide yet another mechanism to explain the common association of ilmenite rims around lunar armalcolites.

## INTRODUCTION

Armalcrite,  $(\text{Fe,Mg})\text{Ti}_2\text{O}_5$ , seems to be unique to the moon due to the high titanium magma necessary for its formation, but more significantly due to the low oxygen fugacity required during crystallization to keep all its iron in the ferrous state (Anderson et al., 1970). Thus, anything we can learn about armalcrite stability should prove valuable in determining lunar petrologic conditions. To this end there have been several papers dealing with this subject, and much of the work has been done or summarized by Lindsley et al. (1974) and Kesson and Lindsley (1975).

It is known that pseudobrookite solid solutions, of which armalcrite is a member, break down with decreasing temperature or increasing pressure to an ilmenite solid solution plus rutile (Haggerty and Lindsley, 1970; Lindsley et al., 1974). Therefore, since armalcrite occurs as a liquidus phase in lunar mare rocks, a knowledge of its high pressure stability should provide information about the depth of origin of these basalts.

Haggerty (1973) divided armalcrites into three groups based on zirconium content. The first is Zr-free with  $\text{Fe}/(\text{Fe}+\text{Mg})$  ratios variable around 0.5 and characteristic of the high-titanium mare basalts. The second is a Cr-Zr-Ca-armalcrite, and the third is Zr-armalcrite; these last two are characteristic of the high-alumina, non-mare basalts. Therefore, because of the very different lunar environments in which all three of these are found, an

investigation was made to determine any difference in stability due to the presence or absence of zirconium in synthetic armalcolites.

In addition, the stability of armalcolite as a function of oxygen fugacity can provide a useful indicator of the limiting conditions of oxidation on the moon during the crystallization of lunar basalts. A knowledge of the range of  $fO_2$  under which armalcolite is stable and of the equilibrium oxide mineral assemblages outside this range provides important information about lunar cooling histories in terms of  $fO_2$ . The work of Usselman and Lofgren (1976) indicates that the presence of a silicate liquid does not change the  $fO_2$  stability of armalcolite.

#### EXPERIMENTAL TECHNIQUE

All of the experiments in this study were done using synthetic materials. The armalcolites produced were characterized chemically by microprobe analyses, and structurally by X-ray powder diffraction. These materials were similar to published descriptions of lunar armalcolites in all respects, except possibly the degree of cation ordering. The synthetic material was disordered with respect to iron over the two octahedral cation sites as determined by Mössbauer spectroscopy (Virgo, personal communication); whereas lunar armalcolite may be ordered (Lind and Housley, 1972; Smyth, 1974). This difference in ordering means that the materials will have a slightly different free entropy at room temperature, but this should have

little effect on the stability either as a function of total pressure or  $fO_2$  at elevated temperatures.

The materials used in the high pressure study were synthesized from reagent grade: Fe-metal,  $Fe_2O_3$ ,  $MgO$ ,  $TiO_2$ , and  $ZrO_2$  using sealed double silica glass capsules with finely powdered iron between them as an oxygen "getter" (Lindsley et al., 1974). Homogeneous mixtures of the reagent powders were fired for ten days, reground, and fired for seven more days at  $1300^\circ C$ . This procedure produced a phase-pure armalcolite with the exception of traces of rutile (estimated optically to be less than 1%) probably due to the presence of some ferric iron.

Zirconium-armalcolites were prepared by weighing in 4% and 10%  $ZrO_2$  for  $TiO_2$  on a molar basis and firing as described above. However, both charges produced armalcolite containing 4%  $ZrO_2$  by microprobe analysis. The excess  $ZrO_2$  in the sample with 10% initially was presumably lost to the glass, which was devitrified and showed traces of zircon in the X-ray pattern, (no zircon was observed in the sample).

High pressure experiments were done in the piston-cylinder apparatus at the Goddard Space Flight Center after calibration against the melting point of gold. Unbuffered runs were made in  $Ag_{60}Pd_{40}$  capsules and three such capsules, each containing a sample of different composition, were run at the same time in the press. These capsules were in a vertical position in an equilateral configuration with the sides touching each other and all void spaces filled with crushable alumina to act as the pressure transmitting medium. This

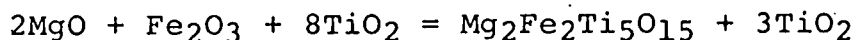


configuration presumably allowed three compositions to be run under identical conditions, but to check this assumption, three capsules, each containing the same composition, were run together. Upon quenching, all three contained a three-phase assemblage in which the amounts of each phase estimated by X-ray diffraction intensities were constant among the three charges. Runs were held at the temperature and pressure of interest for one hour; reversed runs were held for one hour at a pressure above the nearest phase boundary and then dropped to the point of interest and held for one more hour.

To determine the stability of armalcolite as a function of oxygen fugacity, a thermogravimetric technique was employed, see Fig. This technique is similar to that used by Taylor (1964) on the system:  $\text{FeO-Fe}_2\text{O}_3\text{-TiO}_2$ . In a reaction involving only the gain or loss of oxygen from iron oxide constituents, the weight change is a direct measure of the degree of completion of the reaction. Achievement of constant weight is an indication that a redox equilibrium has been reached, and the final weight is a measure of the equilibrium composition, providing no material other than oxygen is removed. A known starting composition, therefore, can be subjected to a stream of flowing gas of known  $f\text{O}_2$  at any given temperature, and the weight change at constant temperature will reflect the equilibrium composition at that  $f\text{O}_2$ . The temperature chosen for this study was  $1200^\circ\text{C}$ , because it is approximately the temperature at which lunar armalcolite crystallizes according to remelt studies of lunar rocks; e.g.,

Akimoto et al., (1970). This method has the advantage of measuring composition under the desired experimental conditions; i.e., temperature and  $fO_2$ , without having to resort to quenching, except as desired for confirmation of phase assemblages.

The starting materials for this gravimetric experiment were reagent grade:  $MgO$ ,  $Fe_2O_3$ , and  $TiO_2$  in weighed proportions corresponding to a magnesium-rich keneddyite plus rutile as follows:



These oxides were mixed in a mechanical shaker, pressed into pellets in a 1 cm. die, and then sintered. It was determined that a pressure of about 10,000 p.s.i. produced the best pellets. At significantly higher or lower pressures the pellets tended to crumble. The pellets were then sintered in silica glass capsules in air. Various combinations of temperature and time were tried, but 800°C for 24 hrs. proved to be the best combination and produced porous pellets which reacted quickly with the gas.

Several of these pellets (usually 1-2 gms.) were suspended in the furnace by a platinum wire attached to an alumina rod, which, in turn, was connected by a wire to the arm of an analytical balance set above the furnace. The weight change associated with this reaction going to completion is 1.82%; therefore, starting with a 2 gm. sample and a sensitivity of 0.0001 gm., the precision of this measurement is about  $\pm 0.3\%$ . The  $fO_2$  in the furnace was controlled by a  $CO_2/H_2$  gaseous buffer and was measured with a  $Y_2O_3$ -stabilized  $ZrO_2$  oxygen fugacity sensor such as described by Sato (1971). The weight change was recorded as a

function of  $fO_2$  and equilibrium was usually achieved in less than six hours. Several runs were cycled by reduction and subsequent reoxidation, and these returned to their original weight, indicating that no material other than oxygen was lost or gained by the sample. Other runs were quenched to check the phases present.

The precision of the cell is  $\pm 0.01$  log units based on the 1 mv. precision of the readout, which is stable within 1 mv. over 24 hrs. This, of course, also implies stability of the gas mixing ratio, and this stability was repeatedly observed. The greatest error in this system, therefore, arises from the precision of the temperature measurement. A radial temperature gradient of  $5^\circ C$  was observed in the furnace under the experimental conditions, and this temperature difference produces a change in  $fO_2$  of 0.07 log units. Maximum errors of  $\pm 5^\circ C$  in temperature and  $\pm 0.1$  log units  $fO_2$  therefore seem reasonable.

Those samples that were quenched were analyzed by X-ray diffraction to determine the phases present, and some samples were also analyzed with the microprobe. In addition, two samples were analyzed by Dr. D. Virgo using the Mössbauer apparatus at the Geophysical Laboratory of the Carnegie Institution.

## RESULTS

### High Pressure

In order to check the suitability of silver-palladium capsules for the pressure runs, one of the quenched capsules was analyzed with the microprobe. The capsule chosen was one of  $Ag_{55}Pd_{45}$  alloy from a 1 hr. run at  $1200^\circ C$  and 10 kb. The inner

surface in contact with the charge was recovered and analyzed, and the results indicate that iron loss to silver-palladium amounted to 0.21% of the sample weight. This loss is 1.4 wt. % of the total iron in the sample and therefore is insignificant. The oxygen liberated by this mechanism must not have greatly affected the sample since no evidence of oxidation was observed in the sample optically, i.e., by an increase in rutile. Alloys richer in silver, used at lower temperatures, should absorb even less iron (Muan, 1963). Any oxidation would appear as an increase in the field of stability of armalcolite (Haggerty and Lindsley, 1970) and thus be reported as a higher value for the depth of formation of these rocks.

Three armalcolite compositions were used, each with a 0.5 Fe/(Fe + Mg) ratio initially. Composition I contained no zirconium; compositions II and III were those prepared with 4% and 10% by weight  $\text{ZrO}_2$ . The microprobe analyses of these materials along with the unit cell parameters determined from a least-squares refinement of X-ray powder diffraction data are given in Table 1. Data are also tabulated for some of the materials prepared at known  $f\text{O}_2$  and quenched from the controlled atmosphere furnace, including a zirconium-armalcolite (Comp. V) prepared thermogravimetrically, for comparison with compositions II and III. The powder diffraction data were indexed according to the orthorhombic space group, Bbmm with the cell refinement program developed by Evans et al., (1963). It may be seen that  $\text{ZrO}_2$  content is approximately equal for compositions

II and III indicating that perhaps 4%  $\text{ZrO}_2$  is a saturation value for armalcolite under these conditions of preparation. It can also be seen that the "a" parameter is the most sensitive to zirconium content.

With increasing pressure, armalcolite breaks down to a more magnesian armalcolite plus ilmenite solid solution plus rutile, as predicted by Lindsley et al., (1974). With further increase in pressure,  $\text{ilmenite}_{\text{ss}}$  plus rutile becomes the stable phase assemblage. This breakdown is shown schematically in Fig. 2. The actual P-T decomposition curves are given in Fig. 3 for composition I (Zr-free armalcolite), and, for compositions II and III (Zr-armalcolites) which produced identical results.

All runs were in the piston-out mode at 1000°C, 1100°C, and 1200°C, and all runs in the three- and one-phase regions were also reversed. However, it became apparent that equilibrium was not being attained at 1000°C; therefore, the curves are drawn from the more precisely determined points at 1200°C through those at 1100°C to the 1 atmosphere breakdown points determined by Lindsley et al., (1974) for armalcolite with 0.5 Fe/(Fe + Mg) molar composition and no zirconium. Two points at 1000°C and 8 kb lie outside the curves as drawn, but these were discounted due to the equilibrium problems at this lower temperature. The data are given in Table 2.

It can be seen that zirconium has the effect of decreasing armalcolite stability, but this effect is not great. It was not possible to probe each breakdown assemblage due to the

finely intergrown textures produced. However, the zirconium-armalcolites in all cases contained less of the armalcolite phase than the Zr-free materials in three-phase regions. In those cases where some of the decomposition products could be analyzed it was found that the zirconium partitioned approximately equally into both the rutile and ilmenite solid solution. The highest  $\text{ZrO}_2$  content found was 6 wt.% in rutile with the average around 4 wt.% in rutile and ilmenite. The rutile also contained a maximum of 4 wt.% FeO and 2 wt.% MgO, but adequate data could not be obtained on the small grains to evaluate the effect of temperature and pressure on these solubilities. It is probable, however, that increased pressure has the effect of increasing  $\text{ZrO}_2$  solubility in ilmenite over the values reported for lunar ilmenites at 1 atm. by Taylor and McCallister (1972).

#### Redox Stability

The stability of armalcolite as a function of oxygen fugacity is indicated by the equilibrium weight loss curve in Fig. 4. In this plot the ordinate shows the percentage of the calculated weight loss corresponding to stoichiometric armalcolite. Therefore, the origin corresponds to the starting composition ( $\text{Mg}_2\text{Fe}_2\text{Ti}_5\text{O}_{15} + 3\text{TiO}_2$ ), in which all iron is ferric, and the 100% point corresponds to  $\text{Mg}_2\text{Fe}_2\text{Ti}_4\text{O}_{10}$ , in which all iron is ferrous--an actual weight loss of 1.82%. The total weight loss curve, therefore, shows the composition in equilibrium with any given  $f\text{O}_2$  at  $1200^\circ\text{C}$ . The compositions of the samples prepared by approaching from more reducing conditions

were the same as those approached from oxidizing conditions, and constant weight was achieved in less than 6 hrs. for reduction and less than 2 hrs. for oxidation.

From this thermogravimetric analysis it can be seen that the starting material at  $1200^{\circ}$  begins to reduce even in  $\text{CO}_2$  ( $f_{\text{O}_2} = 10^{-3.5}$  atm.) and continues until about  $10^{-9.5}$  atm.  $f_{\text{O}_2}$ . The curvature over this  $f_{\text{O}_2}$  range (i.e., a to b in Fig. 4) is caused by the changing ratios of the activities in the solid solution, and this solid solution was confirmed by X-ray diffraction of the quenched runs. Armalcolite as a single phase is then stable over a range of  $f_{\text{O}_2}$  from  $10^{-9.5}$  to  $10^{-10.5}$  atm., (see b to c in Fig. 4) indicating a range of stoichiometry, and this behavior would be predicted by the configuration of the oxygen isobars in the analagous system:  $\text{FeO-Fe}_2\text{O}_3\text{-TiO}_2$  (Taylor, 1964).

As the oxygen fugacity is lowered beyond the  $10^{-10.5}$  atm. limit, weight loss continues (c to d in Fig. 4) until  $10^{-12.8}$  atm., which is the most reducing condition which could be produced without allowing hydrogen to ignite at the top of the furnace. At this oxygen fugacity the weight loss is 125% of that calculated to produce stoichiometric armalcolite and corresponds to an actual weight loss of 2.27% of the starting material. The break in slope of this curve indicates a phase change, and its continuation beyond 100%, the point at which all iron is ferrous, indicates that reduction is still continuing, and either ferrous iron is reduced to metal and/or  $\text{Ti}^{4+}$  is reduced to  $\text{Ti}^{3+}$ .

When the quenched samples were examined under reflected light and by X-ray diffraction, it was found that nothing other than the pseudobrookite solid solution plus rutile was formed at oxygen fugacities greater than  $10^{-9}$  atm. Those prepared between  $10^{-9.5}$  and  $10^{-10.5}$  atm. contained only single phase armalcolite, while those at  $10^{-12.2}$  and  $10^{-12.8}$  atm. consisted of armalcolite plus ilmenite.

The technique described above produces a well-crystallized armalcolite (from the sharpness of the X-ray peaks) of known composition, and free from the contamination problems associated with preparations in metal containers such as molybdenum or even preparations in silica glass. For this reason, an attempt was made to synthesize a zirconium-armalcolite and a calcium-zirconium-armalcolite by this same technique for comparison with similar lunar materials.

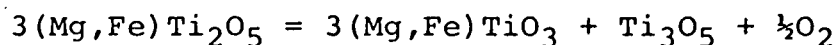
Mixtures were prepared as before, but with 5%  $ZrO_2$  by weight substituting for  $TiO_2$ , and a second mixture with 5%  $ZrO_2$  substituting for  $TiO_2$  and with 3%  $CaO$  substituting for  $MgO$ . These were fired at  $1200^{\circ}C$  and  $10^{-10.5}$  atm.  $fO_2$ , at which point weight losses observed corresponded to the reduction of all ferric iron to ferrous. The product of the run with 5%  $ZrO_2$  was a chemically homogeneous armalcolite containing 4%  $ZrO_2$  plus finely dispersed  $ZrO_2$  grains (presumably 1%). The run with  $CaO$  and  $ZrO_2$  produced a pseudobrookite solid solution containing 2%  $ZrO_2$ , no  $CaO$  in the pseudobrookite material, plus another unidentified phase rich in both  $Ca$  and  $Zr$ .



It therefore appears that 4%  $\text{ZrO}_2$  saturates armalcolite prepared by this technique as well as that previously described (double silica capsules). It further appears that the presence of  $\text{CaO}$  produces a second titanate phase, rich in zirconium, and that these zirconium-bearing materials are stable under the same conditions of oxidation as zirconium-free armalcolite. The calculated and observed X-ray patterns for synthetic armalcolite and zirconium-armalcolite prepared by this technique are given in Tables 3 and 4.

Mössbauer data were obtained on the zirconium-free material from runs at  $1200^\circ\text{C}$  and  $10^{-10.5}$  and at  $10^{-12.8}$  atm.  $f\text{O}_2$ , and these revealed no  $\text{Fe}^{3+}$  nor  $\text{Fe}^0$ . If, therefore, the weight loss from  $10^{-10.5}$  to  $10^{-12.8}$  is ascribed to the reduction of titanium, then about 7 mole %  $\text{Ti}_3\text{O}_5$  must be formed, probably in solid solution with armalcolite. In addition, ilmenite solid solution is formed to maintain the bulk composition (except for the oxygen component).

The data, therefore, indicate that armalcolite is stable over a range of  $f\text{O}_2$  of at least an order of magnitude around  $10^{-10}$  atm. at  $1200^\circ\text{C}$ , and through this range, composition is relatively insensitive to  $f\text{O}_2$ . At lower  $f\text{O}_2$ ,  $\text{Ti}^{4+}$  is reduced to  $\text{Ti}^{3+}$  according to the following reaction:



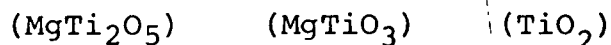
This reaction was only measured as far as 7 mole %  $\text{Ti}_3\text{O}_5$ , but it is probable that upon further reduction (below  $10^{-12.8}$  atm. at  $1200^\circ$ ), iron is reduced to metal. It is also probable that some

of the  $\text{Ti}^{3+}$  enters the ilmenite as a  $\text{Ti}_2\text{O}_3$  component, which would be consistent with the data of Woermann and Lamprecht (personal communication) on the magnesium-free system Fe-Ti-O.

### Lunar Implications

Since armalcolite appears to be a liquidus phase, Fig. 5 shows the intersection of the armalcolite P-T stability curves with a region containing the P-T liquidus curves for Apollo 11 and 17 high-titanium mare basalts as determined experimentally by others, Ringwood and Essene (1970), Green, et al. (1975), Kesson (1975), Akimoto, et al. (1970), and Papike, et al. (1974). Also shown are the curves for the breakdown reactions which take place with rising pressure:

(i) Karrooite  $\rightarrow$  geikielite + rutile



(ii) Ferropseudobrookite  $\rightarrow$  ilmenite + rutile



The curve for the former reaction is drawn from the data of Lindsley et al. (1974). The curve for the latter is drawn from the breakdown temperature of  $\text{FeTi}_2\text{O}_5$ , determined as  $1140^\circ\text{C}$  at 1 atm. by Haggerty and Lindsley (1970), to a point which is indicated by the convergence of the P-T curves determined at lower temperatures. This convergence suggests that all four solid state reaction curves probably cross over in a rather narrow p-t region, if not at a point. The cross-over is very close to the lunar liquidus and indicates that rocks containing

armalcolite of 0.5Fe/(Fe+Mg) molar ratio must have crystallized near the liquidus below the curve separating the one- and three-phase regions. Thus the maximum pressure at which armalcolite could reasonably crystallize as a liquidus phase corresponds to a depth on the moon of about 400 km. Kesson and Lindsley (1975) have shown that the addition of trivalent cations such as  $\text{Al}^{3+}$ ,  $\text{Cr}^{3+}$ , and  $\text{Ti}^{3+}$  stabilize armalcolite to lower temperatures, and increased pressure increases the breakdown temperature of these materials by  $35^{\circ}\text{C}/\text{kb}$ , compared with  $20^{\circ}\text{C}/\text{kb}$  determined for the materials in this study.

The effect of zirconium is apparently the opposite from that of the trivalent cations, but in any case 400 km. remains a maximum crystallization depth for armalcolite. At this depth, the isobaric cooling range throughout which armalcolite would be a stable phase would be very narrow, but, in fact, crystallization probably takes place at much shallower depths. It is also possible, of course, that the ilmenite and rutile which are commonly associated with armalcolite in lunar basalts could be formed by reactions other than that related to the breakdown of armalcolite. Ilmenite (without rutile) surrounding armalcolite probably formed by a different mechanism; however, these pressures should place an upper limit on the depth at the time of crystallization of armalcolite-bearing lunar rocks.

This study also confirms the stability of a zirconium-armalcolite under lunar conditions and explains the 4% maximum observed in this type of lunar material. However, the data

indicate that Ca-Zr-armalcolite probably does not exist on the moon, but that materials of this composition are probably phases with a structure different from that of armalcolite, or a mixture of finely intergrown phases.

The equilibrium  $fO_2$  for armalcolite, determined in this study at 1 atm. is several orders of magnitude more oxidizing than that determined for lunar basalts by Sato et al. (1973), and increased total pressure affects the value for armalcolite only slightly (+0.25 log units at 10 kb.). It is therefore apparent that armalcolite on the moon must be more reduced than pure  $(Fe^{2+}, Mg^{2+})Ti_2^{4+}O_5$ . Specifically, the synthetic samples prepared at 1200°C and  $10^{-12.2}$  and  $10^{-12.8}$  atm.  $fO_2$  fall within the range of lunar oxygen fugacities determined by Sato, and the weight loss in these samples corresponds to  $Ti_3O_5$  contents of 5.4 mole % and 7.0 mole % respectively. This range of  $Ti_3O_5$  contents compares with the 4% - 10% determined for lunar armalcolites by Wechsler et al. (1975) from a recalculation of microprobe analyses to bring the total cation/anion ratio to 3.5. Trivalent titanium must therefore be significant on the moon and must form before metallic iron upon reduction.

Reduction may also provide a mechanism for the formation of ilmenite rims around armalcolite. While there are many explanations for these, at present the most satisfactory is a reaction of armalcolite with FeO in the liquid to produce a more iron-rich armalcolite plus ilmenite. This is discussed by Papike et al. (1974) and El Goresy et al. (1974). It is,

however, possible that these rims formed by reduction upon cooling while still above the solidus. Usselman et al. (1975, 1976) in studies on synthetic high-titanium basalts found ilmenite rims around armalcolite at oxygen fugacities similar to those determined by Sato, et al. (1973) for lunar basalts. However, at lower oxygen fugacities (1.4 log units below the iron-wustite buffer), these rims were not present, probably because this is in the region in which iron metal forms upon reduction instead of ilmenite. Such reduction could be accomplished, as suggested by Sato, et al. (1973) and Sato (1976), by the loss of sulfur as the magma was extruded into the high vacuum lunar environment, or possibly by minute flakes of graphite in the rock. It may also be accomplished by hydrogen implanted by the solar wind and released as basaltic magma flowed over the lunar regolith (Mao et al., 1974). It is apparent, though, that most lunar basaltic magmas have been reduced either during ascent or extrusion, and this reduction would affect the surface of early crystallized armalcolite thereby forming ilmenite plus a  $\text{Ti}^{3+}$ -rich armalcolite.

Lunar armalcolites have been reported to be ordered with respect to titanium vs. (iron + magnesium) (Lind and Housley, 1972; Smyth, 1974). However, this ordering probably occurred below the solidus in an armalcolite which was disordered when it crystallized originally from the magma, Wechsler, et al. (1976). It is therefore likely that lunar armalcolites were no more ordered when they crystallized than those prepared in the present study.

## SUMMARY AND CONCLUSIONS

Synthetic armalcolite and zirconium-armalcolite were prepared and characterized. These phases break down with increasing pressure to an assemblage of ilmenite solid solution plus rutile. The effect of zirconium in armalcolite is to decrease the P-T field of stability through breakdown at slightly higher temperatures. A comparison of the P-T curves determined in this study with mare basalt liquids indicates that the armalcolite-bearing rocks could not have crystallized at a depth greater than about 400 km. on the moon. Further, armalcolite in equilibrium at oxygen fugacities typical of lunar basalts must contain iron present only as  $\text{Fe}^{2+}$  plus significant amounts of  $\text{Ti}^{3+}$  (5-7 mole %  $\text{Ti}_2\text{O}_3$ ). Ilmenite rims commonly present around lunar armalcolite crystals could have resulted from the reduction of armalcolite phenocrysts, while still above the solidus.

## ACKNOWLEDGMENTS

We wish to acknowledge NASA and Dr. C. Schnetzler and J. Weidner for allowing us to use the high pressure apparatus at the Goddard Space Flight Center, and Dr. D. Virgo for the use of the Mössbauer apparatus at the Geophysical Lab. of the Carnegie Institution. In addition, we would like to acknowledge helpful discussions with Drs. A.M. Gaines, D. H. Lindsley, S.E. Kesson, A. El Goresy, S.E. Haggerty, and E. Woermann. This work was supported in part by NASA grants NSG 7031 and NSG 7119, and a grant from the Penrose Fund of the Geol. Soc. of America.

## REFERENCES

- AKIMOTO S., NISHIKAWA M., NAKAMURA Y., KUSHIRO I., AND KATSURA T.  
(1970) Melting experiments of lunar crystalline rocks. Proc. Apollo 11 Lunar Sci. Conf., Geochim. Cosmochim. Acta Suppl. 1, 129-133. Pergamon Press.
- ANDERSON A.T., BUNCH T.E., CAMERON E.M., HAGGERTY S.E., BOYD F.R., FINGER L.W., JAMES O.B., KEIL K., PRINZ M., RAMDOHR P., and EL GORESY A. (1970) Armalcolite: A new mineral from the Apollo 11 samples. Proc. Apollo 11 Lunar Sci. Conf., Geochim. Cosmochim. Acta Suppl. 1, 55-63. Pergamon Press.
- EL GORESY A., RAMDOHR P., MEDENBACH O., and BURNHARDT H. (1974) Taurus-Littrow  $\text{TiO}_2$ -rich basalts: opaque mineralogy and geochemistry. Proc. Fifth Lunar Sci. Conf., Geochim. Cosmochim. Acta Suppl. 5, 627-652. Pergamon Press.
- EVANS H., APPELMAN D., and HANDWERKER D. (1963) The least-squares refinement of crystal unit cells with powder diffraction data by an automatic computer indexing method (abs.) Amer. Crystallographic Assoc., Cambridge, Mass. Annual Meeting Prog. 42-43.
- GREEN D.H., RINGWOOD A.E., HIBBERSON W.O., and WARE N.G. (1975) Experimental petrology of Apollo 17 mare basalts. Proc. Sixth Lunar Sci. Conf. Geochim. Cosmochim. Acta. Suppl. 6, 871-893. Pergamon Press.
- HAGGERTY S.E. (1973) Armalcolite and genetically associated opaque minerals in the lunar samples. Proc. Fourth Lunar Sci. Conf., Geochim. Cosmochim. Acta Suppl. 4, 777-797. Pergamon Press.

- HAGGERTY S.E., and LINDSLEY D.H. (1970) Stability of the pseudobrookite ( $\text{Fe}_2\text{TiO}_5$ )-ferropseudobrookite ( $\text{FeTi}_2\text{O}_5$ ) series. Carnegie Inst. Wash. Yearbook 69, 247-249.
- KESSON S.E. (1975) Mare basalts: melting experiments and petrogenetic interpretation. Proc. Sixth Lunar Sci. Conf. Geochim. Cosmochim. Acta Suppl. 6, 921-944. Pergamon Press.
- KESSON S.E., and LINDSLEY D.H. (1975) The effects of  $\text{Al}^{3+}$ ,  $\text{Cr}^{3+}$ , and  $\text{Ti}^{3+}$  on the stability of armalcolite. Proc. Sixth Lunar Sci. Conf., Geochim. Cosmochim. Acta Suppl. 6, 911-920. Pergamon Press.
- LIND M.D., and HOUSLEY R.M. (1972) Crystallization studies of lunar igneous rocks: crystal structure of synthetic armalcolite. Science 175, 521-523.
- LINDSLEY D.H., KESSON S.E., HARTZMAN M.J., and CUSHMAN M.K. (1974) The stability of armalcolite: experimental studies in the system:  $\text{MgO-Fe-Ti-O}$ . Proc. Fifth Lunar Sci. Conf., Geochim. Cosmochim. Acta Suppl. 5, 521-534. Pergamon Press.
- MAO H.K., EL GORESY A., and BELL P.M. (1974) Evidence of extensive chemical reduction in lunar regolith samples from the Apollo 17 site. Proc. Fifth Lunar Sci. Conf., Geochim. Cosmochim. Acta Suppl. 5, 673-683. Pergamon Press.
- MUAN A. (1963) Silver-paladium alloys as crucible materials in studies of low melting iron silicates. Ceram. Bull 42, 344-347.
- PAPIKE J.J., BENICE A.E., and LINDSLEY D.H. (1974) Mare basalts from the Taurus-Littrow region of the moon. Proc. Fifth Lunar Sci. Conf., Geochim. Cosmochim. Acta Suppl. 5, 471-504. Pergamon Press.



- RINGWOOD A.E., and ESSENE E. (1970) Petrogenesis of Apollo 11 basalts, internal constitution and origin of the moon. Proc. Apollo 11 Lunar Sci. Conf., Geochim. Cosmochim. Acta Suppl. 1, 769-799. Pergamon Press.
- SATO M. (1971) Solid electrolyte fugacity sensors. in Research Techniques for High Pressure and High Temperature, G.C. Ulmer ed., Springer-Verlag.
- SATO M. (1976) Oxygen fugacity values of some Apollo 16 and 17 rocks. Lunar Science VII, 758-760. Lunar Science Institute.
- SATO M., HICKLING N.L., and MC LANE J.E. (1973) Oxygen fugacity values for Apollo 12, 14, and 15 lunar samples and reduced state of lunar magmas. Proc. Fourth Lunar Sci. Conf., Geochim. Cosmochim. Acta Suppl. 4, 1061-1079. Pergamon Press.
- TAYLOR L.A., and MC CALLISTER R.H. (1972) An experimental investigation of the significance of zirconium partitioning in lunar ilmenite and ulvospinel. Earth Planet. Sci. Lett. 17, 105-109.
- TAYLOR R.W. (1964) Phase equilibria in the system:  $\text{FeO-Fe}_2\text{O}_3\text{-TiO}_2$  at  $1300^\circ\text{C}$ . Amer. Mineral. 49, 1016-1030.
- SMYTH J.R. (1974) The crystal chemistry of armalcolites from Apollo 17. Earth Planet. Sci. Lett. 24, 262-270.
- USSELMAN T.M., and LOFGREN G.E. (1976) Phase relations of high-titanium mare basalts as a function of oxygen fugacity. Lunar Science VII, 888-890. Lunar Science Institute.
- USSELMAN T.M., LOFGREN G.E., DONALDSON C.H., and WILLIAMS R.J. (1975) Experimentally reproduced textures and mineral chemistries of high-titanium mare basalts. Proc. Sixth Lunar Sci. Conf., Geochim. Cosmochim. Acta Suppl. 6, 997-1020. Pergamon Press.

WECHSLER B.A., PREWITT C.T., and PAPIKE J.J. (1975) Structure and chemistry of lunar and synthetic armalcolite. Lunar Science VI, 860-862. Lunar Science Institute.

WECHSLER BA.A., PREWITT C.T., and PAPIKE J.J. (1976) Chemistry and structure of lunar and synthetic armalcolite. Earth and Planetary Sci. Letters 29, 91-103.

Table 1

Composition of starting materials	Equipment	Microprobe analysis (wt.%)				Powder Diffraction Unit Cell Dimensions (Å)			
		MgO	FeO	TiO <sub>2</sub>	ZrO <sub>2</sub>	TOTAL	a	b	c vol.
I (arm.)	Press	8.11	14.93	76.89	0.09	100.02	9.73	10.05	3.74 366
II (Zr-arm)	Press	8.13	15.02	72.95	3.85	99.95	9.78	10.04	3.76 369
III (Zr-arm)	Press	8.17	15.03	73.18	4.03	100.41	9.78	10.04	3.75 368
IV (arm)	C.A.F.*	9.36	16.14	73.92	0.05	99.47	9.77	10.02	3.75 367
V (Zr-arm)	C.A.F.*	9.31	15.86	70.85	3.86	99.88	9.80	10.04	3.75 369

\*C.A.F. = Controlled-atmosphere furnace (see Fig.1)

Table 2. Conditions, starting compositions and results of runs at elevated pressures and temperatures.

TEMPERATURE	PRESSURE	STARTING COMPOSITIONS		
		I	II	III
		PRODUCTS		
		$\Phi/\% \text{arm.}$	$\Phi/\% \text{arm.}$	$\Phi/\% \text{arm.}$
1200°C	15 kb.↑	R+I	R+I	R+I
	14 kb.↑	R+I	R+I	R+I
	13 kb.↑	R+I+A/30		
	11 kb.↑	R+I+A/70	R+I+A/40	R+I+A/50
	10 kb.↑	A	R+I+A/80	R+I+A/80
	5 kb.↓	A	A	A
	10 kb.↓	A	R+I+A/80	R+I+A/70
	11 kb.↓	R+I+A/70	R+I+A/50	R+I+A/50
1100°C	12 kb.↑	R+I		
	11 kb.↑		R+I	R+I
	9 kb.↑	R+I+A/50	R+I+A/40	R+I+A/40
	6 kb.↑	R+I+A/90	R+I+A/80	R+I+A/70
	5 kb.↓	A		
	6 kb.↓	R+I+A/90	R+I+A/70	R+I+A/70
	9 kb.↓	R+I+A/40	R+I+A/40	R+I+A/40
1000°C	11 kb.↑	R+I		
	9 kb.↑		R+I	R+I
	8 kb.↑	R+I+A/10	R+I+A/10	
	3 kb.↑	R+I+A/80	R+I+A/70	R+I+A/70
	3 kb.↓	R+I+A/70	R+I+A/60	R+I+A/60

Compositions:

I Armalcolite 0.5Fe/Mg + Fe

II Armalcolite 0.5Fe/Mg + Fe (4% wt. substitution of Zr for Ti)

III Armalcolite 0.5Fe/Mg + Fe (10% wt. substitution of Zr for Ti)

Products:

R = rutile

I = ilmenite

A = armalcolite

% arm. = percentage of armalcolite in 3 phase assemblages as estimated from relative X-ray peak heights.

↑ = points approached from lower pressure

↓ = points approached from higher pressure

Φ = phases present

Table 3. Synthetic Armalcolite X-ray Pattern

hkl	d(obs.)	d(calc.)	I/I <sub>0</sub>
020	5.0200	5.0105	20
200			
101	4.8900	4.8853	60
220	3.5000	3.4979	50
230	2.7575	2.7574	100
301	2.4557	2.4578	15
400	2.4415	2.4426	15
131	2.4149	2.4157	15
240	2.2286	2.2292	15
420	2.1953	2.1956	25
430	1.9713	1.9717	20
002	1.8725	1.8731	10
250	1.8546	1.8542	10
341	1.7552	1.7545	10
060	1.6698	1.6702	25
610	1.6075	1.6073	5
312	1.6034	1.6028	5
351	1.5532	1.5532	20

Preparation: 1200°C,  $fO_2 = 10^{-10.5}$  atm.

Analysis (wt.%): MgO 9.36 (Fe<sub>.5</sub>Mg<sub>.5</sub>)Ti<sub>2</sub>O<sub>5</sub>  
 (microprobe) FeO 16.14  
 TiO<sub>2</sub> 73.97  
 99.47

X-ray conditions: Cu/Ni K $\alpha$  radiation. 45KV, 15ma.  
 Philips powder diffractometer  
 scan down from 60° 2 $\theta$  at ½°/min.  
 internal Si standard  
 indexed with least-squares computer  
 program to orthorhombic space  
 group Bbmm using 16 peaks

a 9.77 ±.01  
 b 10.02 ±.01  
 c 3.75 ±.01  
 vol. 366.8 ±1

Table 4. Synthetic Zr-Armalcolite X-ray Pattern

hkl	d(obs.)	d(calc.)	I/I <sub>0</sub>
020	5.0300	5.0183	25
200	4.9200	4.9011	40
101	3.5100	3.5063	75
220	2.7660	2.7631	100
230	2.4660	2.4622	25
301	2.4531	2.4505	25
400	2.4190	2.4180	30
131	2.2317	2.2334	30
240	2.1994	2.2020	50
420	1.9752	1.9769	30
430	1.8581	1.8575	15
250	1.7552	1.7574	10
341	1.6732	1.6728	25
060	1.6407	1.6413	15
521	1.5532	1.5528	20
351			

Preparation: 1200°C,  $fO_2 = 10^{-10.5}$  atm.

Analysis (wt.%): MgO 9.31 (Fe<sub>.5</sub>Mg<sub>.5</sub>)Ti<sub>1.9</sub>Zr<sub>.105</sub>  
 (microprobe) FeO 15.86  
 TiO<sub>2</sub> 70.85  
 ZrO<sub>2</sub> 3.86  
 99.88

X-ray conditions: Cu/Ni K $\alpha$  radiation. 45KV, 15ma.  
 Philips powder diffractometer  
 scan down from 60° 2 $\theta$  at ½°/min.  
 internal Si standard  
 indexed with least-squares computer  
 program to orthorhombic space  
 group Bbmm using 15 peaks.

a 9.80 ±.01  
 b 10.04 ±.01  
 c 3.75 ±.01  
 vol. 368.9 ±1

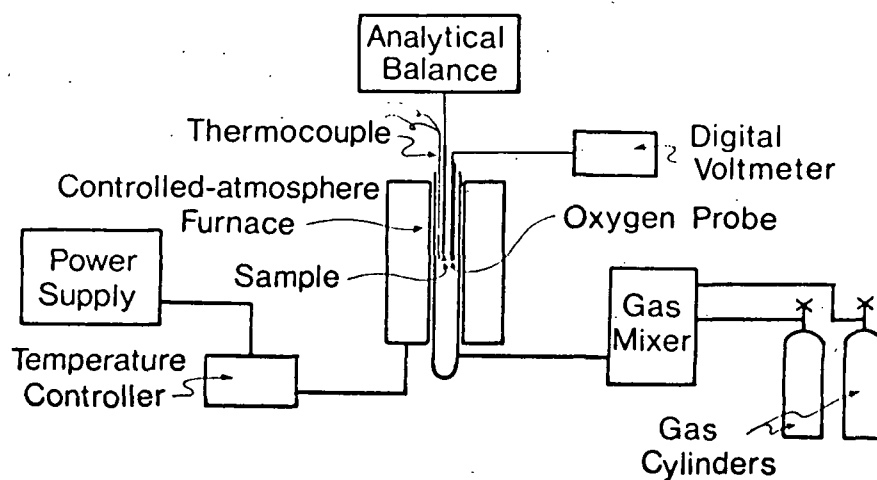


Fig. 1. Schematic diagram of system for thermogravimetry at controlled oxygen fugacities and at one atmosphere total pressure.

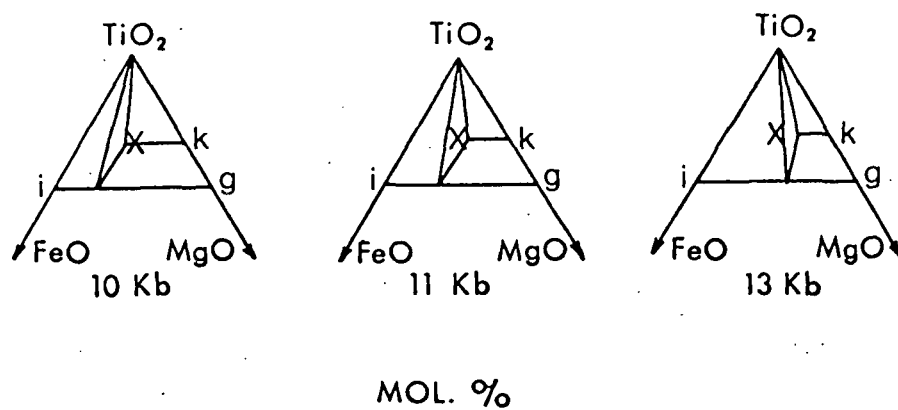


Fig. 2. Schematic illustration of the stages of isothermal ( $1200^\circ\text{C}$ ) decomposition of  $\text{MgFeTi}_4\text{O}_{10}$  with rising pressure. X = Fixed bulk composition ( $\text{MgO} \cdot \text{FeO} \cdot 4\text{TiO}_2$ ). i = ilmenite ( $\text{FeTiO}_3$ ), g = geikielite ( $\text{MgTiO}_3$ ), k = karrooite ( $\text{MgTi}_2\text{O}_5$ )



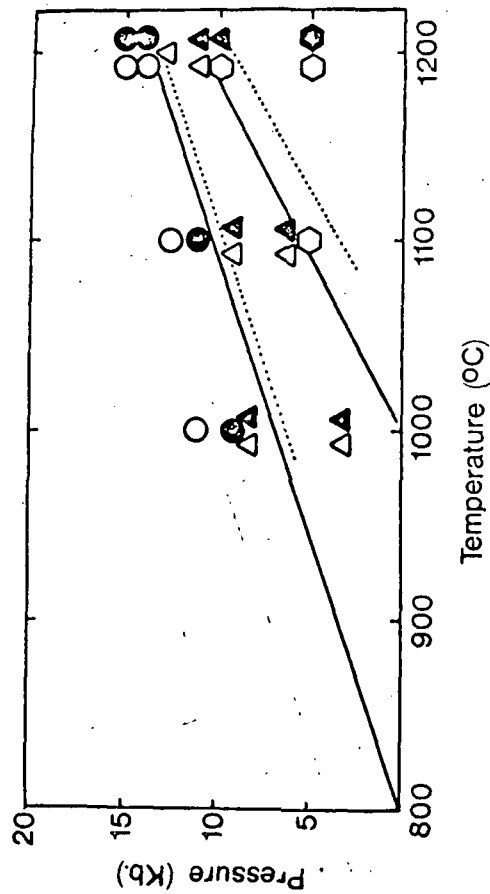


Fig. 3. Results of experiments with Zr-doped (solid symbols) and Zr-free (open symbols) armalcolite compositions at elevated pressures and temperatures.

● and ○ Single phase armalcolite ( $\text{Fe}/(\text{Fe}+\text{Mg})=0.5$ , molar basis)

⊙ and ○ Rutile + ilmenite solid solution

▲ and △ Rutile + ilmenite (solid solution) + armalcolite ( $\text{Fe}/\text{Fe}+\text{Mg} < 0.5$ )

Continuous lines are boundaries between zirconium-free phase assemblages. Dotted lines indicate probable boundaries between phase assemblages with 4 wt. %  $\text{ZrO}_2$  (replacing  $\text{TiO}_2$  on a molar basis in armalcolite).

See text for data interpretation at 1000°C.

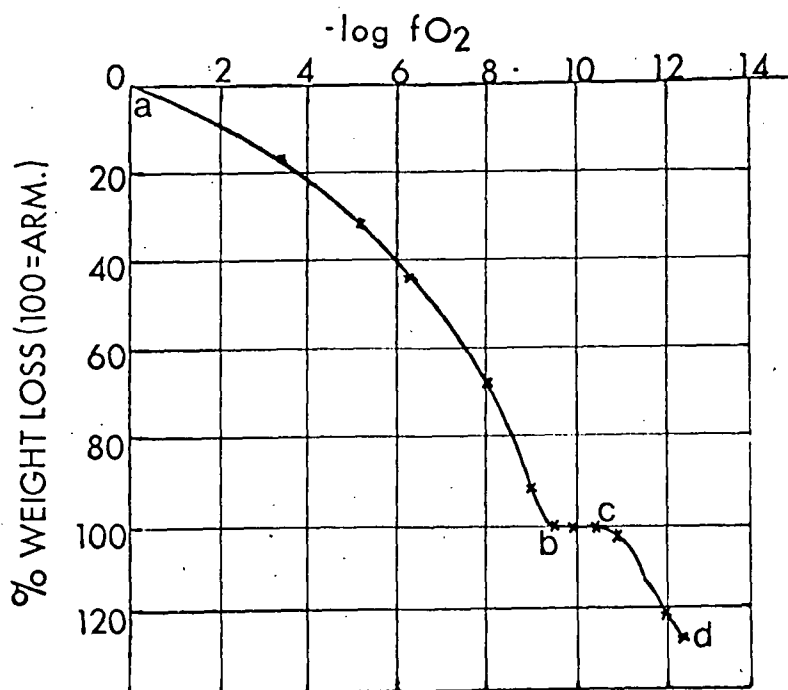


Fig. 4. Thermogravimetric stability curve for 1:1:4 (Mg:Fe:Ti) oxide compositions as a function of oxygen fugacity at 1200°C.

Stable phases: a to b, Magnesian pseudobrookite-armalcolite solid solutions + rutile.

b to c, Armalcolite ( $\text{MgFeTi}_4\text{O}_{10}$ ).

c to d and beyond, Reduced armalcolite + ilmenite.

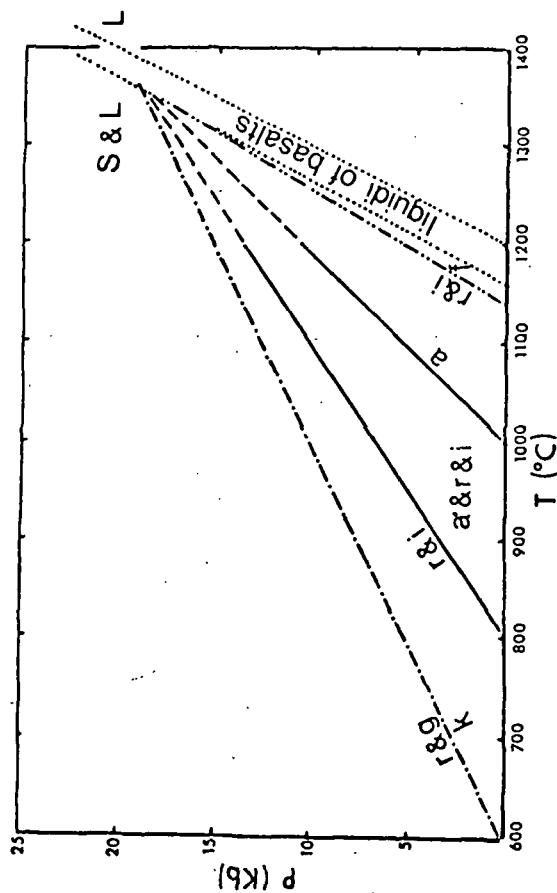


Fig. 5. Phase equilibria in the  $\text{MgTiO}_3$  -  $\text{FeTiO}_3$  -  $\text{TiO}_2$  system at elevated pressures and temperatures.  $r$  = rutile,  $g$  = geikielite,  $k$  = karrooite,  $i$  = ilmenite,  $a$  = armalcolite ( $\text{MgFeTi}_4\text{O}_{10}$ ),  $a'$  = armalcolite ( $\text{Fe}/(\text{Fe}+\text{Mg}) < 0.5$ ).  $S$  = Solid,  $L$  = Liquid. The curve for  $r + g \rightleftharpoons k$  (---) is from Lindsley et al., (1974)